AD-A163 297 THREE-DIMENSIONAL NUMERICAL SIMULATIONS OF FELS BY TRANSVERSE MODE SPECTRAL METHOD(U) NAVAL RESEARCH LAB WASHINGTON DC C TANG ET AL. 30 DEC 85 NRL-MR-5694 1/1

UNCLASSIFIED F/G 20/5 NL

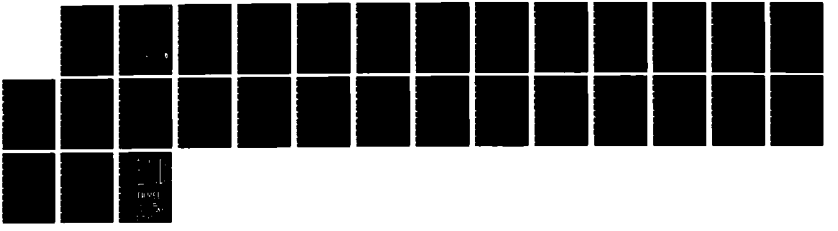

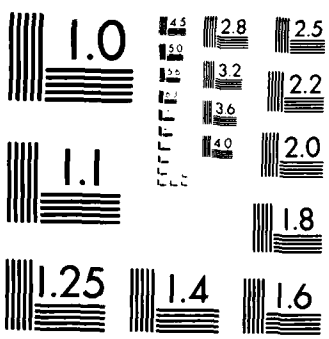

NRL Memorandum Report 5694

Three-Dimensional Numerical Simulations of FELs by Transverse Mode Spectral Method

CHA-MEI TANG AND P. SPRANGLE

Plasma Theory Branch
Plasma Physics Division

December 30, 1985

NAVAL RESEARCH LABORATORY
Washington, D.C.

AD-A163 247

SECURITY CLASSIFICATION OF THIS PAGE

REPORT DOCUMENTATION PAGE

1a. REPORT SECURITY CLASSIFICATION UNCLASSIFIED	1b. RESTRICTIVE MARKINGS
2a. SECURITY CLASSIFICATION AUTHORITY	3. DISTRIBUTION / AVAILABILITY OF REPORT Approved for public release; distribution unlimited.
2b. DECLASSIFICATION / DOWNGRADING SCHEDULE	
4. PERFORMING ORGANIZATION REPORT NUMBER(S) NRL Memorandum Report 5694	5. MONITORING ORGANIZATION REPORT NUMBER(S)
6a. NAME OF PERFORMING ORGANIZATION Naval Research Laboratory 6b. OFFICE SYMBOL (If applicable) Code 4790	7a. NAME OF MONITORING ORGANIZATION
6c. ADDRESS (City, State, and ZIP Code) Washington, DC 20375-5000	7b. ADDRESS (City, State, and ZIP Code)
8a. NAME OF FUNDING / SPONSORING ORGANIZATION DARPA 8b. OFFICE SYMBOL (If applicable)	9. PROCUREMENT INSTRUMENT IDENTIFICATION NUMBER
8c. ADDRESS (City, State, and ZIP Code) Arlington, VA 22209	10. SOURCE OF FUNDING NUMBERS PROGRAM ELEMENT NO. 62702E; PROJECT NO. 5483; TASK NO.; WORK UNIT ACCESSION NO. DN155-384

11. TITLE (Include Security Classification)

Three-Dimensional Numerical Simulations of FELs by Transverse Mode Spectral Method

12. PERSONAL AUTHOR(S)
Tang, Cha-Mei and Sprangle, P.

13a. TYPE OF REPORT	13b. TIME COVERED	14. DATE OF REPORT (Year, Month, Day)	15. PAGE COUNT
Interim	FROM _____ TO _____	1985 December 30	29

16. SUPPLEMENTARY NOTATION

17. COSATI CODES			18. SUBJECT TERMS (Continue on reverse if necessary and identify by block number)
FIELD	GROUP	SUB-GROUP	Numerical methods for FELs Self-focusing in FELs FEL

19. ABSTRACT (Continue on reverse if necessary and identify by block number)

We present a numerical method for solving a three-dimensional radiation field by decomposing the radiation field into transverse modes that satisfy the free space wave equation and the boundary conditions. The formalism includes betatron oscillations in a realizable wiggler, finite emittance and energy spread in an amplifier or oscillator configuration. This formalism can be generalized to calculate sidebands resulting from the synchrotron oscillations. The transverse mode spectral method is compared with the finite difference method, spectral method and transform spectral method. Examples from a computer code using Gaussian-Hermite expansion are given. We show self-focusing of the radiation beam due to gain and refraction of the FEL.

20. DISTRIBUTION / AVAILABILITY OF ABSTRACT ☒ UNCLASSIFIED/UNLIMITED ☐ SAME AS RPT. ☐ DTIC USERS	21. ABSTRACT SECURITY CLASSIFICATION UNCLASSIFIED
22a. NAME OF RESPONSIBLE INDIVIDUAL Cha-Mei Tang	22b. TELEPHONE (Include Area Code) (202) 767-4148 22c. OFFICE SYMBOL Code 4790

DD FORM 1473, 84 MAR 83 APR edition may be used until exhausted. All other editions are obsolete.

SECURITY CLASSIFICATION OF THIS PAGE

CONTENTS

THREE-DIMENSIONAL NUMERICAL SIMULATIONS OF FELS BY TRANSVERSE MODE SPECTRAL METHOD

I. INTRODUCTION

Three-dimensional simulations of the FEL gain process will become increasingly important in the design, optimization and interpretation of FEL experiments. Since the fundamental FEL concepts have been successfully demonstrated, the FEL is now pushing the limits of the FEL capabilities in all directions. Due to the increasing complexity of FEL experiments, simple one-dimensional theory is often not adequate. At the same time, however, the analytical three-dimensional results are only obtainable for a limited number of special operating conditions. The importance of the three-dimensional effects will vary with the experiments. Some examples of the three-dimensional effects that need to be understood are:

(a) The transverse electron beam profile is often asymmetric, resulting in the asymmetry of the radiation field. This is most pronounced in the storage rings and circular microtrons.

(b) The radiation field varies both in the transverse and axial directions. There is a crucial trade-off of large filling factors with short Rayleigh lengths and vise versa. The optimal situation varies with the experiments.

(c) Betatron oscillations from the wiggler field cause electrons to sample a varying radiation field. Under certain situations, this can cause betatron-synchrotron instabilities.

(d) FELs are pushing toward high gain operation. Strong self-focusing in a high gain FEL can substantially alter the wave front properties. A resonator, not self-consistly designed with FEL physics, most likely is not the optimal design for the high gain FEL operation.

(e) Sideband instabilities in an oscillator can lead to pulse breakup and affect the quality of the radiation beam.

The analytical and numerical methods employed in the study of the transverse variation of the wave equation have taken the approaches of transverse mode spectral method.[1-5]

Manuscript approved September 18, 1985.

transform spectral method,[6,7] spectral method,[2] finite difference method,[8,9] and Lienard-Wiechert potential method[10]. The different methods refer to the techniques used to evaluate the $\nabla_\perp^2 \mathbf{A}_R$ term in the wave equation, where $\mathbf{A}_R$ is the vector potential of the radiation field. All three kinds of spectral methods involve representing the solution of the radiation field as a truncated series of known functions of the independent variables.

The transverse mode spectral method decomposes the radiation field into a truncated series of a complete set of orthogonal functions, which satisfy the free space wave equations with the appropriate boundary conditions. One takes advantage of the transverse mode properties to reduce the wave equation to a set of first order differential equations.

For the spectral method and transverse spectral method, the series takes on the form of a transform, and the wave equation reduces to a simple form in the transformed variables, i.e., $\nabla_\perp^2 \mathbf{A}_R$ has an analytical form in the transform space. The transform spectral method requires numerically taking the transform of the driving current. The spectral methods describe the current in terms of the Lagrangian variables, and the current term can be evaluated analytically.

In Sec. II, we will outline the transverse mode spectral method in general, i.e., not specifying the form of the transverse modes. This formulation will include slow transverse motion and betatron oscillations of the electrons in the realistic wiggler, finite emittance, energy spread and self-consistent axial particle dynamics. This method conserves energy. The formalism is extended to the study of sideband formation[1-2,11-12] on a long electron pulse in the FEL oscillator.

In Sec. III, we outline the spectral and the transverse spectral methods. The three different spectral methods are compared in this section.

The advantages of the transverse mode spectral method are: i) Free space wave propagation, finite size mirrors, and apertures can be handled analytically. ii) It is easy to include transverse particle motion exactly. iii) This method lends itself to analytical and semi-analytical solutions and can provide physical insight for many problems. iv) The transverse boundary conditions are included automatically in the waveguide mode expansion.

In Sec. IV, we apply the transverse mode spectral method to an example with self-focusing properties. In this example the electron beam focuses due to gain and refraction.[13-17]

II. THE TRANSVERSE MODE SPECTRAL METHOD

A. THE WAVE EQUATION

In this paper, we will consider only the linearly polarized wiggler, since that is the most common wiggler field. The formulation for a circularly polarized wiggler requires only minor modifications. The realistic magnetic field will be expressed in terms of the vector potential of the wiggler,

$$\mathbf{A}_w(y,z) = \bar{A}_w(y,z)\cos(\int_0^z k_w(z')dz')\hat{\mathbf{e}}_x, \tag{1}$$

where $\bar{A}_w(y,z) = A_w(z)\cosh(k_w y)$, $A_w(z)$ and $k_w(z)$ are the slowly varying amplitude and wavenumber of the wiggler.

When $k_w y << 1$, one can use the approximation $\bar{A}_w \sim A_w(z)$ for the calculation of gain and axial particle dynamics. The accurate form for $\bar{A}_w$ is only necessary in the calculation of the betatron oscillations. For convenience, we define a dimensionless wiggler parameter $K(z) = (|e|/\sqrt{2}m_o c^2)A_w(z)$.

We also include a DC accelerating electric field,[14] $E_{DC}\hat{e}_z$, for the purpose of efficiency enchancement. For convenience, we define a dimensionless parameter $e_{DC} = |e|E_{DC}/m_o c^2$.

The radiation field will be expressed as

$$\mathbf{A}_R(x,y,z,t) = -\mathbf{A}(x,y,z)\frac{\exp[i(kz-\omega t)]}{2} + c.c., \tag{2}$$

where

$$\mathbf{A}(x,y,z) = A_x(x,y,z)\hat{\mathbf{e}}_x + A_y(x,y,z)\hat{\mathbf{e}}_y = \sum_{\ell=0}^{L}\sum_{m=0}^{M} A_{\ell,m}(z)\hat{\mathbf{e}}_{\ell,m}(x,y,z)e^{i\beta_{\ell,m}z}.$$

$$\hat{\mathbf{e}}_{\ell,m} = G_{\ell,m}\hat{\mathbf{e}}_x + F_{\ell,m}\hat{\mathbf{e}}_y$$

is the general form of the transverse mode. $A_{\ell,m} = |A_{\ell,m}|e^{i\varphi_{\ell,m}}$ is the complex amplitude of the normal modes, $G_{\ell,m} = g_{\ell,m}e^{i\theta_{\ell,m}}$ represents the x-component of the complex transverse mode. $F_{\ell,m}$ is the y-component of the complex transverse mode. (which may be zero.) $A_x(x,y,z) = |A_x(x,y,z)|\exp(i\varphi(x,y,z))$, and $k = \omega/c$. We use lower case to denote the

normalized parameters of the radiation field, such as $a_x(x,y,z) = (|e|/\sqrt{2}m_oc^2)A_x(x,y,z)$ and $a_{\ell,m} = (|e|/\sqrt{2}m_oc^2)A_{\ell,m}$.

The function $\grave{\mathbf{e}}_{\ell,m}(x,y,z)$ should satisfy the free space wave equation and the appropriate boundary conditions, i.e.,

$$\left(\nabla_\perp^2 + \frac{\partial^2}{\partial z^2} - \frac{1}{c^2}\frac{\partial^2}{\partial t^2}\right)\grave{\mathbf{e}}_{\ell,m}(x,y,z)e^{i\beta_{\ell,m}z}e^{i(kz-\omega t)} \simeq 0. \tag{3}$$

The orthogonality condition is

$$\int\int \grave{\mathbf{e}}_{\ell,m}\cdot\grave{\mathbf{e}}^*_{\ell',m'}dxdy = \delta_{\ell,\ell'}\delta_{m,m'}, \tag{4}$$

where the integration is over the appropriate radiation domain.

The wave equation for the FEL is

$$\left(\nabla_\perp^2 + \frac{\partial^2}{\partial z^2} - \frac{1}{c^2}\frac{\partial^2}{\partial t^2}\right)\mathbf{A}_R = -\frac{4\pi}{c}\mathbf{J}_\perp. \tag{5}$$

Substituting the expression of the radiation field into the wave equation, and making the slowly varying approximation, we obtain

$$\sum_{\ell,m} 2ik\frac{\partial A_{\ell,m}}{\partial z}e^{i\beta_{\ell,m}z}e^{i(kz-\omega t)}\grave{\mathbf{e}}_{\ell,m} + c.c. = -\frac{8\pi}{c}\mathbf{J}_\perp. \tag{6}$$

Multiply both sides of Eq. (6) by $\exp(-i(kz-\omega t))$ and integrate in time over a period. Then, dot both sides by $\grave{\mathbf{e}}^*_{\ell,m}$ and integrate over the transverse dimension. The result is

$$\frac{\partial A_{\ell,m}}{\partial z} = -\frac{i}{k}\frac{4\pi}{c}\int_0^{2\pi/\omega}\frac{dt}{2\pi/\omega}\int dx\int dy J_z G^*_{\ell,m}e^{-i\beta_{\ell,m}z}e^{-i(kz-\omega t)}. \tag{7}$$

Now we need to evaluate the current. The fluid-like electron density is

$$D(x,y,z,p_x,p_y,p_z,t) = d_o(x_o,y_o,p_{x,o},p_{y,o},p_{z,o},\psi_o)\delta(x-\tilde{x})\delta(y-\tilde{y})\frac{\delta(t-\tau)}{|\partial\tilde{z}/\partial t|}$$

$$\delta(p_x-\tilde{p}_x)\delta(p_y-\tilde{p}_y)\delta(p_z-\tilde{p}_z). \tag{8}$$

The variables with "$\sim$" and the variable τ are functions of the Lagrangian variables $x_o, y_o, p_{x,o}, p_{y,o}, p_{z,o}, \psi_o, z$, where x_o, y_o are the initial transverse positions at the entrance of the wiggler $z=0$, $p_{x,o}, p_{y,o}$ are the initial transverse momentums at $z=0$, $p_{z,o}$ is the initial axial momentum spread at $z=0$, $\psi_o = -\omega t_o$ is the initial phase of the electron in

the ponderomotive potential well, t_o is the time the electrons enter the wiggler at $z = 0$, and τ is the time that the electron reaches position z. The function d_o is the initial phase space density distribution, including the effects of emittance and energy spread.

The fluid-like beam density can be defined as

$$n(x, y, z, t) = \int_{\infty}^{\infty} dp_x \int_{\infty}^{\infty} dp_y \int_{\infty}^{\infty} dp_z D(x, y, z, p_x, p_y, p_z, t). \tag{9}$$

We will define the effective area of the electron beam to be

$$\sigma_b(z, t) = \frac{1}{n_o} \int dx \int dy \;\; n(x, y, z, t), \tag{10}$$

where $n_o = n(x, y, z, t)|_{max}$.

The current density can be defined as

$$\begin{aligned} J_x &= -|e| v_{zo} \int dp_x \int dp_y \int dp_z D(x, y, z, p_x, p_y, p_z, t) \frac{p_x}{\gamma m_o} \\ &= -|e| n_o v_{zo} \int d\psi_o \int dx_o \int dy_o \int dp_{x,o} \int dp_{y,o} \int dp_{z,o} \\ &\frac{\tilde{p}_x}{\tilde{p}_z} \frac{1}{n_o} d_o(x_o, y_o, p_{x,o}, p_{y,o}, p_{z,o}, \psi_o) \delta(x - \tilde{x}) \delta(y - \tilde{y}) \delta(t - \tau). \end{aligned} \tag{11}$$

The final form of the wave equation is

$$\frac{da_{\ell,m}}{dz} = iCF_1(z) K(z) \left\langle \frac{G^*_{\ell,m}(\tilde{x}, \tilde{y}, z) \exp(-i\psi) \exp(-i\beta_{\ell,m} z)}{\tilde{\gamma} \tilde{\beta}_z} \right\rangle, \tag{12}$$

where

$$\begin{aligned} < \ldots >= \int_0^{2\pi} \frac{d\psi_o}{2\pi} \int_{-\infty}^{\infty} dx_o \int_{-\infty}^{\infty} dy_o \int_{-\infty}^{\infty} dp_{x,o} \int_{-\infty}^{\infty} dp_{y,o} \int_0^{\infty} dp_{z,o} \\ (\ldots) \frac{1}{n_o \sigma_b} d_o(x_o, y_o, p_{x,o}, p_{y,o}, p_{z,o}, \psi_o) \end{aligned} \tag{13}$$

is the ensemble average, the normalization is $< (1) >= 1$, $C = (\omega_b^2/c^2)(\beta_{zo}/2k)\sigma_b$, $\omega_b = (4\pi|e|^2 n_o/m_o)^{1/2}$, $F_1(z) = J_o(b) - J_1(b)$ comes from the fast electron oscillation in the z-direction due to the linearly polarized wiggler, $b(z) = K^2/2(1 + K^2)$, $\psi = \int_0^z (k_w(z') + k - \omega/\tilde{v}_z) dz' + \psi_o$, $\tilde{\beta}_z = \tilde{v}_z/c$. $\beta_{zo} = v_{zo}/c$. and v_{zo} is the mean initial axial velocity.

B. PARTICLE DYNAMICS

The mean transverse particle position and momentum, in general, should be integrated along with the axial particle momentum equations. Under certain circumstances, analytical forms for the transverse particle trajectories are sufficient.

Taking the betatron oscillations as an example, the particle motion in the x-direction, without any additional external focusing, can be written as

$$\tilde{x} = x_o + (p_{xo}/\gamma_o m_o c)z. \tag{14}$$

The particle motion in the y-direction exhibits betatron oscillations. Taking $k_w\tilde{y} << 1$, the particle dynamics in the y-direction[16-17] is approximately

$$\tilde{y} = y_\beta \left(\frac{k_\beta(0)}{k_\beta(z)}\right)^{1/2} \cos\left(\int_0^z k_\beta(z')dz' + \varphi_\beta\right), \tag{15}$$

where $k_\beta = Kk_w/\gamma_o$, $y_\beta = (\bar{p}_{y,o}^2 + y_o^2)^{1/2}$, $\bar{p}_{y,o} = p_{y,o}/k_\beta(0)\gamma_o m_o c^2$, and $\varphi_\beta = \cos^{-1}(y_o/y_\beta)$.

The particle motion in the z-direction is best written in terms of the equation for the total relativistic gamma factor

$$\frac{d\tilde{\gamma}}{dz} = -\frac{k}{\tilde{\gamma}} F_1(z)K(z)|a_z(\tilde{x},\tilde{y},z)|\sin(w + \varphi(\tilde{x},\tilde{y},z)) - e_{DC}, \tag{16}$$

and the equation governing the phase

$$\frac{d^2w}{dz^2} = \frac{(1+\beta_{zo})k_w}{\tilde{\gamma}}\left(\frac{d\tilde{\gamma}}{dz} + e_{DC}\right) + T + \delta B_w, \tag{17}$$

where

$$T = \frac{dk_w}{dz} - \frac{k}{2\tilde{\gamma}^2}\frac{dK^2}{dz} - k\frac{1+K^2}{\tilde{\gamma}^3}e_{DC} \tag{18}$$

is the degree of taper for the efficiency enhancement schemes.

$$\delta B_w = \frac{k}{4\tilde{\gamma}^2} y_\beta^2 \frac{k_\beta(0)}{k_\beta(z)}(1+\cos\Phi)\frac{d\left[K^2(z)k_w^2(z)\right]}{dz} \tag{19}$$

includes the effect resulting from the combination of betatron oscillation and contoured B_w field, and

$$\Phi(y_o, p_{yo}, z) = 2\int_0^z k_\beta(z')dz' + 2\varphi_\beta.$$

Equations (12, 16-17) form the self-consistent set of equations for the radiation field and the particle dynamics.

C. CONSERVATION OF ENERGY

We can show that this formulation conserves energy. To do this, we rewrite Eq. (16) in terms of the amplitude of each mode.

$$\frac{d\tilde{\gamma}}{dz} = -\frac{k}{\tilde{\gamma}} F_1(z) K(z) \sum_{\ell,m} g_{\ell,m}(\tilde{x}, \tilde{y}, z) |a_{\ell,m}(z)| e^{-Im(\beta_{\ell,m})z} \sin \psi_{\ell,m} - e_{DC}. \tag{20}$$

where $\psi_{\ell,m} = \psi + \theta_{\ell,m} + \phi_{\ell,m}$ is the phase associated with each mode. We have assumed here that $Re(\beta_{\ell,m})z << 2\pi$. The spatial rate of change of the total electron beam energy is

$$\begin{aligned} \left\langle m_o c^2 d\tilde{\gamma}/dz \right\rangle = & - DF_1(z) A_w(z) \sum_{\ell,m} |A_{\ell,m}(z)| e^{-Im(\beta_{\ell,m})z} \left\langle \frac{g_{\ell,m}(\tilde{x}, \tilde{y}, z) \sin \psi_{\ell,m}}{\tilde{\gamma} \tilde{\beta}_z} \right\rangle \\ & - \left\langle m_o c^2 e_{DC} \right\rangle, \end{aligned} \tag{21}$$

where $D = (\sigma_b/8\pi)(\omega_b^2/c^2)\beta_{zo}k$. The spatial rate of change in the radiation energy is

$$\frac{dI_R}{dz} = \frac{k^2}{8\pi} \sum_{\ell,m} \frac{d|A_{\ell,m}|^2}{dz} e^{-2Im(\beta_{\ell,m})z}. \tag{22}$$

Applying Eq. (12) to Eq. (22), we can show that the energy is conserved, i.e., the energy gained by the radiation is equal to the energy lost by the electrons plus the energy supplied by the axial DC electric field.

$$\frac{dI_R}{dz} = \left\langle m_o c^2 \frac{d\tilde{\gamma}}{dz} \right\rangle + \left\langle m_o c^2 e_{DC} \right\rangle. \tag{23}$$

D. THE CHOICE OF THE TRANSVERSE MODES OF THE WAVE EQUATION

The choice of the normal modes, however, will depend on the geometry of the FEL of interest. A few examples of the possible choices of the normal eigenmodes are given below:

(a) Gaussian-Hermite expansion allows the most flexibility in the modeling of the FEL physics of interest in an open resonator. The expressions for $\hat{\mathbf{e}}_{\ell,m} = G_{\ell,m}\hat{\mathbf{e}}_z$ are

$$g_{\ell,m} = \frac{1}{\sqrt{\pi 2^{\ell+m-1}\ell!m!}} \frac{1}{w(z)} H_\ell(\bar{x}) H_m(\bar{y}) \exp(-\frac{1}{2}(\bar{x}^2 + \bar{y}^2)), \qquad (24a)$$

$$\theta_{\ell,m} = \frac{1}{2}(\bar{x}^2 + \bar{y}^2)\varsigma - (\ell + m + 1)\tan^{-1}\varsigma. \qquad (24b)$$

where $\bar{x} = \sqrt{2}x/w(z)$, $\bar{y} = \sqrt{2}y/w(z)$, H_ℓ is the Hermite polynomial of the ℓth order. $\varsigma = (z - z_c)/z_o$, z_c is the axial location of the minimum waist, $w(z) = w_o(1 + \varsigma^2)^{1/2}$. w_o is the spot size, and $z_o = w_o^2 k/2$ is the Rayleigh length.

(b) When the electron beam and the resonator system are axially symmetrical, and when the betatron oscillations are not included in the model of the linearly polarized wiggler, then the radiation can be assumed to be axially symmetrical. The Gaussian-Leguerre modes are the choice for the expansion, and each term is expressed as $\hat{\mathbf{e}}_{o,m} = G_{o,m}\hat{\mathbf{e}}_x$, where

$$g_{o,m} = \sqrt{\frac{2}{\pi}} \frac{1}{w(z)} L_m^o(\frac{2r^2}{w^2(z)}) \exp(-\frac{r^2}{w^2(z)}), \qquad (25a)$$

$$\theta_{o,m} = -(2m + 1)\tan^{-1}(\varsigma) + \frac{r^2}{w^2(z)}\varsigma, \qquad (25b)$$

L_m^o is the Laguerre polynomial.

(c) In a low gain oscillator, the best choice would be the eigenmodes of the resonator cavity[18] including the effects of apertures, finite size mirrors and resonator losses. The eigen modes in turn can be written in terms of the appropriate Gaussian-Laguerre or Gaussian-Hermite modes. The advantage of going to the resonator cavity modes is that the losses for the higher order resonator cavity modes increase rapidly with the cavity mode number, such that only a few modes need to be kept in the caluclation. In addition there is no need to calculate the radiation outside the FEL wiggler.

(d) Closed waveguides can be used to confine the radiation beam over a distance long compared to a Rayleigh length. If the waveguide is not rectangular, the vector potential of the waveguide modes generally have both x and y components. For the analysis presented here, we have to assume the transverse guide dimensions are large compared to a radiation wavelength. The theory is also restricted to low-order, low-loss modes whose propagation constants $k + Re(\beta_{\ell,m})$ are nearly equal to the plane-wave value, i.e., $Re(\beta_{\ell,m}) << k$. For wavelengths that are comparable to the waveguide diameters

or when multimode analysis are desired, this method has to be modified slightly to include the different frequencies and axial wavenumbers associated with the different waveguide modes. The formulation should be similar to that described in the Sec. II.F with sidebands.

E. COMPUTATION SPEED

The cost of computation per axial step is spent mainly for the radiation field. The number of operations is $\alpha_1 N_e(L+1)(M+1)$ to integrate Eq. (12), where N_e is the total number of electrons, and α_1 is a numerical constant. The particle orbit equations require $\alpha_2(L+1)(M+1)N_e/N_o$ number of operations to evaluate the radiation field $a_x(\tilde{x},\tilde{y},z)$, and $\alpha_3 N_e$ number of operations for the integration, where N_o is the number of electrons per ponderomotive wave, and α_2 and α_3 are numerical constants. In general, Eq. (16) is faster than Eq. (20), which requires $\alpha_4(L-1)(M+1)N_e$ number of operations.

F. FREQUENCY SIDEBANDS AND PULSE SLIPPAGE

The electron oscillation in the ponderomotive potential well is called the synchrotron oscillation. We define K_{so} to be the synchrotron wavenumber of the electron traveling exactly along the z-axis

$$K_{so} = \left(\frac{2\sqrt{2} k_w k}{\gamma_o^2} \frac{w_o}{w(z)} K(z) |a_{oo}(z)| \right)^{1/2} . \qquad (26)$$

When the intensity of the radiation becomes high, such that the electrons make half a bounce in the wiggler, then sideband frequencies can grow. One-dimensional simulations[12] and three-dimensional simulations[1-2] show that the amplitude of the radiation field becomes chaotic, and the quality of the radiation field becomes degraded.

In order to understand the effect of sidebands on wavefront curvatures, the three-dimensional formulation is necessary. We assume periodic boundary conditions for the radiation field of length ℓ_{eb}, which is chosen to be many times the amplitude modulation distance and the pulse slippage distance. If the length of the electron beam is much longer

than ℓ_{eb}, only a section of a long electron beam needs to be modeled. If the electron beam is shorter than ℓ_{eb}, then the whole pulse shape must be included.

The radiation field can be written as

$$\mathbf{A}_R(x,y,z,t) = -\mathbf{A}(x,y,\xi,t)\frac{\exp(ik\xi)}{2} + c.c., \tag{27}$$

where

$$\mathbf{A}(x,y,\xi,t) = A_x(x,y,z)\hat{\mathbf{e}}_x + A_y(x,y,z)\hat{\mathbf{e}}_y$$
$$= \sum_{n=0}^{N}\sum_{\ell=0}^{L}\sum_{m=0}^{M} A_{\ell,m,n}(t)\hat{\mathbf{e}}_{\ell,m}(x,y,ct)e^{i\beta_{\ell,m}ct}e^{i(\Delta k_n\xi)}$$

is a slowly varying function of position following the radiation pulse, $k = (1+\beta_{zo})(\gamma_o^2/(1+K^2))k_w$ is the resonant wavenumber, $\Delta k_n = (n-1)\delta k$, $\delta k = 2\pi/\ell_{eb}$, and $\xi = z - ct$. $\mathbf{A}(x,y,\xi,t)$ is a slowly varying function of position and time following the radiation pulse.

Following the same procedure outlined in Sec. II.A and II.B, we obtain the self-consistent set of equations for $a_{\ell,m,n}$, $\tilde{\gamma}$ and ψ. The independent Lagrangian variables are $x_o, y_o, p_{x,o}, p_{y,o}, p_{z,o}, \psi_o, \Psi_o, t$, and

$$\frac{1}{c}\frac{da_{\ell,m,n}}{dt} = iCF_1(z)K(z)\left\langle \frac{G^*_{\ell,m}(\tilde{x},\tilde{y},z)\exp -i(\psi+\Delta k_n\tilde{\xi})\exp(i\beta_{\ell,m}z)}{\tilde{\gamma}\tilde{\beta}_z}\right\rangle\Bigg|_{z=ct}. \tag{28}$$

$$\frac{1}{c}\frac{d\tilde{\gamma}}{dt} = -\frac{k}{\tilde{\gamma}}F_1(z)K|a_x(\tilde{x},\tilde{y},\tilde{\xi},t)|\sin(\psi+\varphi(\tilde{x},\tilde{y},\tilde{\xi},t)) - e_{DC}, \tag{29}$$

and

$$\frac{1}{c^2}\frac{d^2\psi}{dt^2} = \frac{(1+\beta_{z0})k_w}{\tilde{\gamma}}\left(\frac{1}{c}\frac{d\tilde{\gamma}}{dt} + e_{DC}\right) + T + \delta B_w, \tag{30}$$

where

$$< \ldots >= \int_0^{2\pi}\frac{d\Psi_o}{2\pi}\int_0^{2\pi}\frac{d\psi_o}{2\pi}\int dx_o\int dy_o\int_{-\infty}^{\infty}dp_{x,o}\int_{-\infty}^{\infty}dp_{y,o}\int_0^{\infty}dp_{z,o}$$

$$(\ldots)\frac{1}{n_o\sigma_b}d_o(x_o,y_o,p_{x,o},p_{y,o},p_{z,o},\psi_o,\Psi_o) \tag{31}$$

is the ensemble average. $\Psi_o = (2\pi/\ell_{eb})\xi_o$, and $0 \le \xi_o < \ell_{eb}$ are the axial location of the electron in the electron pulse at t=0, $\psi = \int_o^t(k_w(ct')+k)\tilde{v}_z dt' - ckt + \psi_o$, $\tilde{z} = \int_o^t \tilde{v}_z dt' + \xi_o$.

$\tilde{\xi} = \bar{z} - ct \simeq \Psi_o/\delta k - s$, and $s = ct(1+K^2)/2\gamma_o^2$ is the pulse slippage distance.

The method described above is straightforward. Since the number of electrons that must be used to model the electron beam with finite emittance and finite length is large, any general numerical method, including this method, requires a considerable amount of computation time. For limited computational resources, it is necessary to form simplified models. This formulation lends itself towards semi-analytical models of finite length electron pulses,[1-2,18] where some of the integrals in the expression for ensemble average can be evaluated analytically.

III. THE SPECTRAL AND TRANSFORM SPECTRAL METHODS

The principle behind the spectral and transform spectral methods is similar to the transverse mode spectral method. The major difference comes from the representation of the radiation field, for example, Fourier series in the Cartesian geometry and Hankel transform in the axially cylindrical geometry.

Let us take the Fourier series for the illustration. The domain for the radiation field is $-D_x/2 \le x \le D_x/2$ and $-D_y/2 \le y \le D_y/2$, and the boundary conditions are periodic. The slowly varying amplitude of the radiation field is written as

$$\mathbf{A}(x,y,z) = \frac{1}{D_x D_y} \sum_{\ell=0}^{L} \sum_{m=0}^{M} A_{\ell,m}(z) e^{i(k_\ell x + k_m y)} \hat{\mathbf{e}}_x, \tag{32}$$

where $k_\ell = 2\pi\ell/D_x$ and $k_m = 2\pi m/D_y$. The equation for the amplitude in terms of the current is

$$\left[\frac{d}{dz} + i\frac{k_\ell^2 + k_m^2}{2k}\right] A_{\ell,m}(z) =$$

$$-\frac{i}{k}\frac{4\pi}{c}\int_0^{2\pi/\omega} \frac{dt}{2\pi/\omega} \int dx \int dy J_z e^{-i(k_\ell x + k_m y)} e^{-i(kz-\omega t)}. \tag{33}$$

When the current J_z is formulated in Eulerian variables for the x and y coordiantes, then the right-hand-side of Eq. (33) has to be evaluated numerically, and the method is called the transform spectral method. If the current is formulated in Lagrangian variables $(x_o, y_o, p_{x,o}, p_{y,o}, p_{z,o}, v_o)$ then Eq. (33) can be reduced to

$$\left[\frac{d}{dz}+i\frac{k_l^2+k_m^2}{2k}\right]A_{l,m}(z)=iCF_1(z)K(z)\left\langle\frac{e^{-i(k_l\tilde{x}+k_m\tilde{y}-\psi)}}{\tilde{\gamma}\tilde{\beta}_z}\right\rangle. \tag{34}$$

The particle dynamics equations (16-17) are also applicable here. For a Fourier series expansion, one can show that the energy is conserved in the D_x by D_y domain for the spectral method.

In general, the Eulerian formulation of the current is inferior to the Lagrangian formulation. The Eulerian formulation is not convenient to use for the study of betatron effects, because the numerical transforms of Eq. (33) require the current to be evaluated at prespecified grids. This problem can be reduced, if the number of grids used across the electron beam is large, which in turn requires a larger number of terms in the expansion. For the Hankel transform, there is the additional problem of numerical errors resulting from numerical integration with a finite number of grids in an infinite integration domain.

The estimate for the speed of computation for the spectral method has the same form as in Sec. II.E. The value for the coefficient α_1, α_2 and α_3 depends on the expansion, and they are smaller for the Fourier transform and larger for the Hankel transform.

The transverse mode spectral method, in some instances, is better than both the spectral and transform spectral methods, because of the following properties. The propagation of the radiation field through apertures, and the reflection and transmission of the radiation field at mirrors can be evaluated in terms of matrix multiplication of the amplitudes of the normal modes. The spectral and transform spectral methods require an additional step in converting the radiation field into Gaussian modes. Finally, the transverse mode spectral method is easier to implement for calculations in complicated waveguide geometries, because the boundary conditions are automatically included.

The transverse mode spectral method is not the best numerical scheme when the FEL wiggler is many times the Rayleigh length and the FEL radiation is strongly focused to the electron beam. The reason is that the higher order modes become more and more important. The number of transverse modes, which have to be included, become large. The Fourier series spectral method employing the Lagrangian Formulation is more appropriate for this type of simulations.

IV. SELF-FOCUSING EXAMPLE AND DISCUSSION

A three-dimensional code employing Gaussian-Hermite expansion of the radiation field is applied to a linearly polarized wiggler. The following examples will show self-focusing properties of the FELs.

The electron beam is assumed to have a Gaussian profile and a radius of 2.25×10^{-2} cm. The current is 50 A and the energy is 109.6 MeV. The wiggler has a magnetic field $B_w = 6.3$ kG, period of 2.4 cm and length $L_w = 6$ m. The incident 0.5 μm radiation at the entrance of the wiggler is a Gaussian TEM_{00} mode with a minimum waist $w_o = 0.06$ cm located at $z = L_w/2$, and a power of 5.8×10^5 W.

In this example, the electron beam radius is much smaller than the spot size, i.e., $r_{eb} << w_o$. If the radiation has the spot size of the electron beam, its Rayleigh length would be only 32 cm. A plot of the power gain is shown in Fig. 1. The FEL is operating in the high gain regime, and the radiation saturates at 4 m.

Figures 2.a-e shows the radiation amplitude at z=0, 150, 300, 450 and 600 cm plotted from $-4w_o$ to $4w_o$ in both the x and y plane. In this example, the self-focusing phenomenon is not only due to refraction, but also gain. The peak amplitude in Figs. 2a-e are 4.5×10^{-2}, 1.1×10^{-2}, 4.6×10^{-2}, 4.1×10^{-2} and 2.6×10^{-2} respectively. At 150 cm, the laser beam is already narrowed down significantly. The corresponding phase front is shown in Fig. 3.a. The focusing due to the electron beam is manifested by the small mound at the center.

The beam radius remains at roughly the same size from 150 cm to the end of the wiggler. Due to electrons oscillating away from the bottom of the ponderomotive potential well, the radiation loses energy after 4 m. In Refs. 13-14, it was shown analytically that FEL radiation is not only governed by gain and diffraction, but also by refraction when operating in the trapped particle mode. For this case, the resonant phase is at the origin, i.e., $\sin \psi_R = 0$. Even though the radiation is losing energy after $z = 4$ m, the radiation beam around the electrons still focuses, while the radiation further away from the electrons defocuses, as shown in Fig. 2.e. This is in qualitative agreement with the theory given by Refs. 13-14. Figure 3.b shows the focusing properties of the wave front. It is important that the radiation beam does not defocus when the radiation is losing energy due to the bouncing of the electrons in the ponderomotive potential well.

The FEL radiation does not always undergo focusing, for example. the electron beam could dig a hole in the laser amplitude profile when the FEL is operating with loss in the low gain regime and large frequency mismatch.

Next. we give an example where the center of the electron beam does not travel down the center of the wiggler due to irregularities in the magnetic wiggler field. The center of the electron beam is assumed to execute a slow sinusoidal motion, $y_{cntr} = r_{eb}\sin(\pi z/L_w)$. The radiation guiding properties of the e-beam is still clearly evident. Fig. 4. The peak amplitude is 2.4×10^{-2}. The motion of the center of the electron beam, however. causes significant distortion of the radiation beam.

In summary, this paper outlines one method of solving the three-dimensional FEL radiation field self-consistently with the electron dynamics. The advantages of this method are: 1) The boundaries in the transverse directions are included automatically. 2) It is easy to incorporate transverse particle motion. 3) Free space prapagation, finite size mirrors and apertures can be handled analytically. 4) This method lends itself to analytical and semi-analytical solutions.

The disadvantages of this method is the increase in the computation time if a large number of electrons are used in the radial direction, and if a large number of modes are required.

The numerical examples illustrate the self-focusing property of the FEL. Under appropriate conditions, the laser radiation maintains a roughly constant radius radiation beam. We also showed that the irregularities in the wiggler field can cause significant distortion of the radiation beam. The implications of this for the FEL design are important. For electron beams with good emittance, it is possible to focus the beam to a small area and operate the FEL in the high gain regime. and not have to worry about diffraction. In this case it is important to design the resonator cavity including the FEL gain model.

Acknowledgment

This work was supported by DARPA under contract No. 5483.

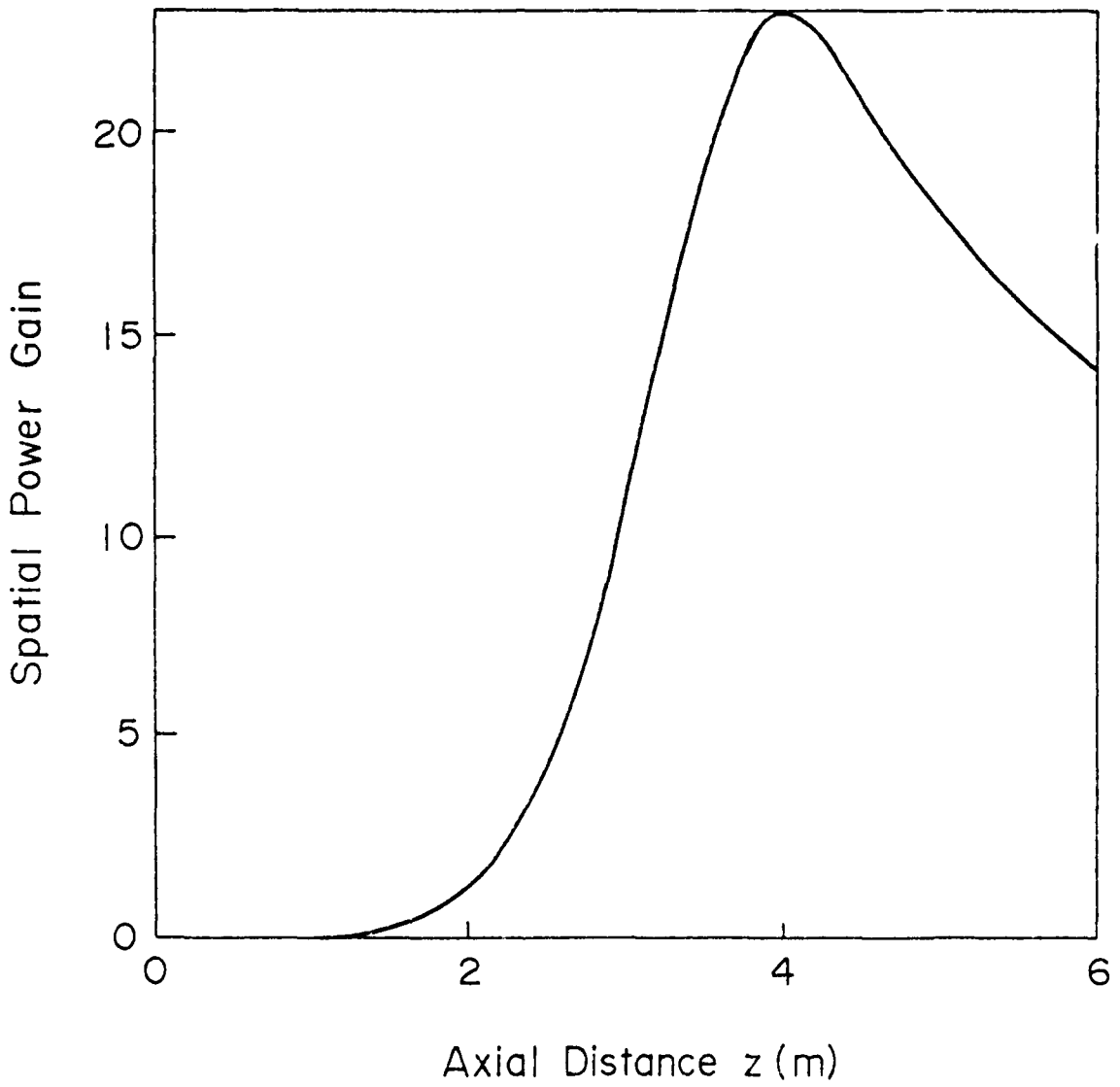

Fig. 1 — A plot of the spatial power gain as a function of axial distance

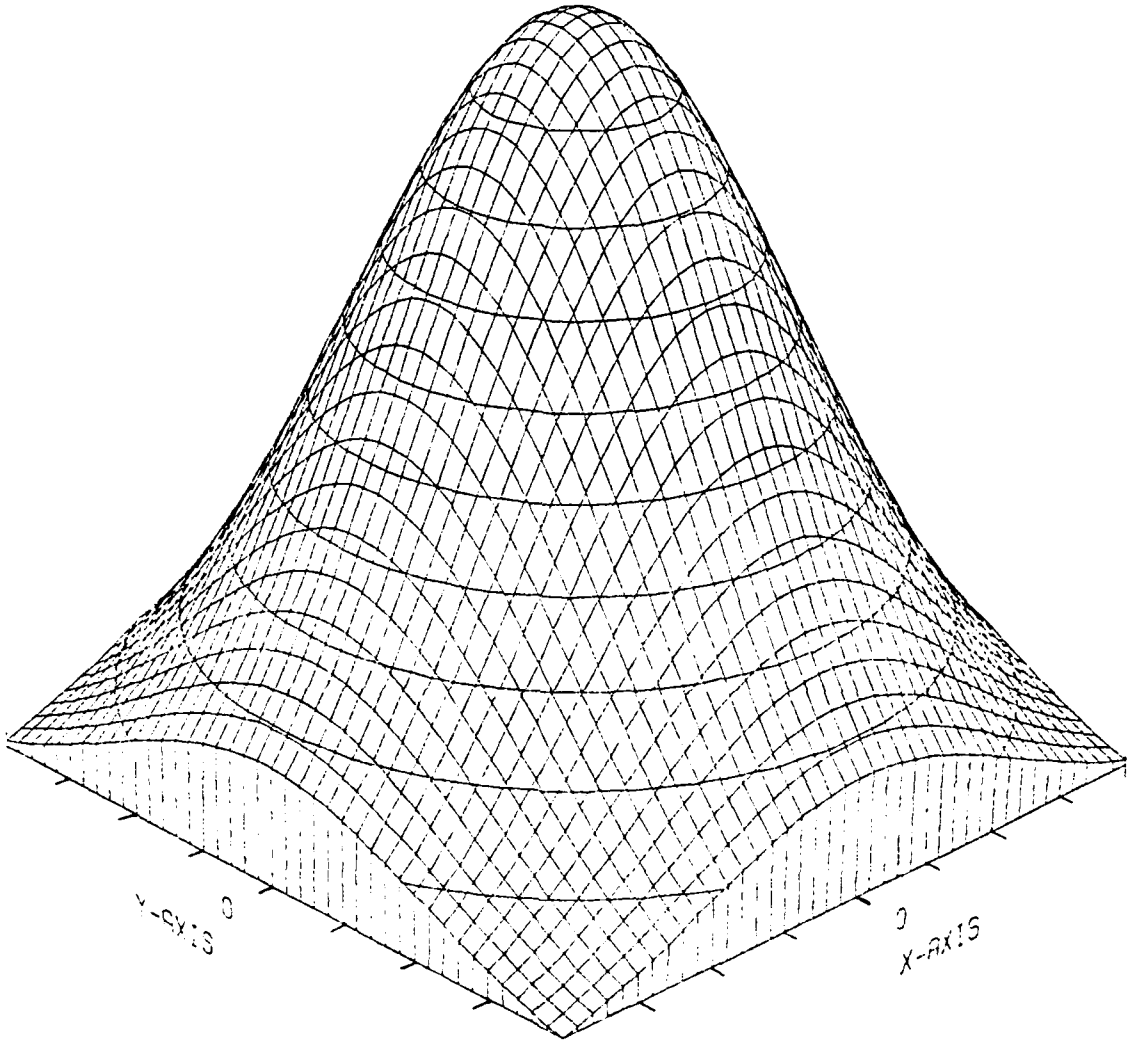

(a)

Fig. 2 — Plots of the amplitude of the radiation field in the x and y plane at (a) z = 0, (b) z = 150 cm, (c) z = 300 cm, (d) z = 450 cm and (e) z = 600 cm. The tick marks are separated by a distance w_g.

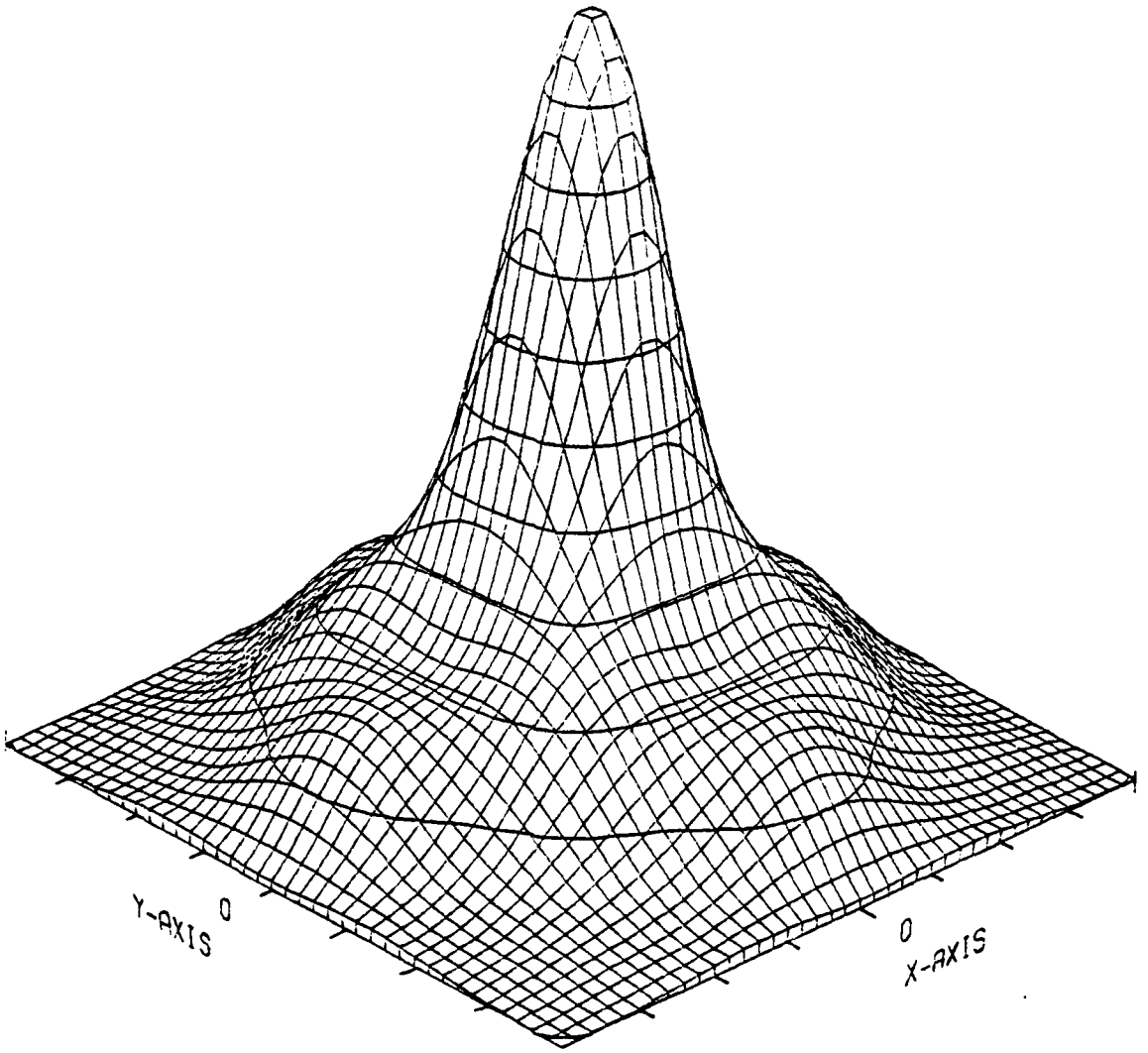

(b)

Fig. 2 (Cont'd) — Plots of the amplitude of the radiation field in the x and y plane at (a) z = 0, (b) z = 150 cm, (c) z = 300 cm, (d) z = 450 cm and (e) z = 600 cm. The tick marks are separated by a distance w_o.

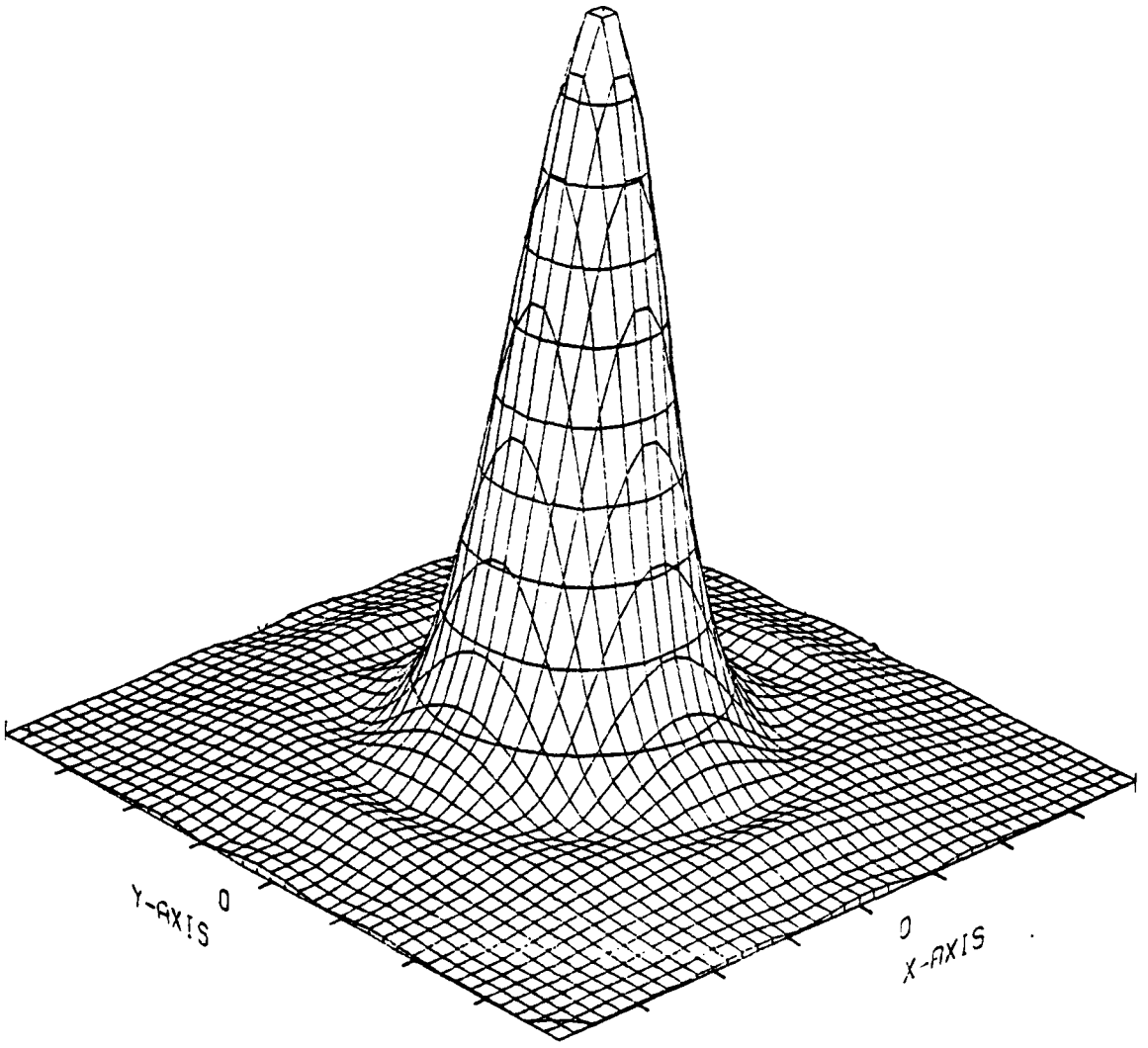

(c)

Fig. 2 (Cont'd) — Plots of the amplitude of the radiation field in the x and y plane at (a) z = 0, (b) z = 150 cm, (c) z = 300 cm, (d) z = 450 cm and (e) z = 600 cm. The tick marks are separated by a distance w_0.

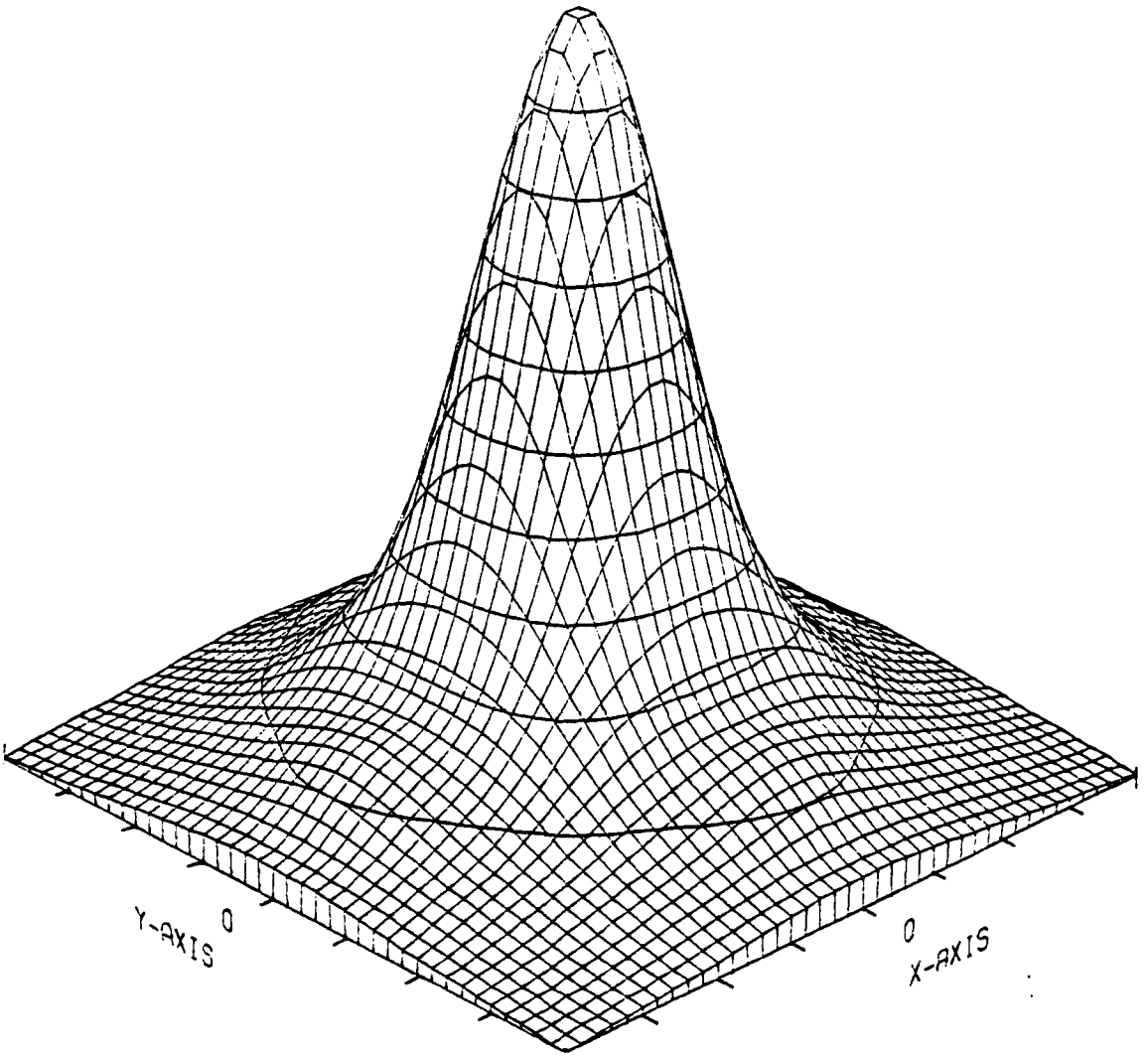

(d)

Fig. 2 (Cont'd) — Plots of the amplitude of the radiation field in the x and y plane at (a) z = 0, (b) z = 150 cm, (c) z = 300 cm, (d) z = 450 cm and (e) z = 600 cm. The tick marks are separated by a distance w_o.

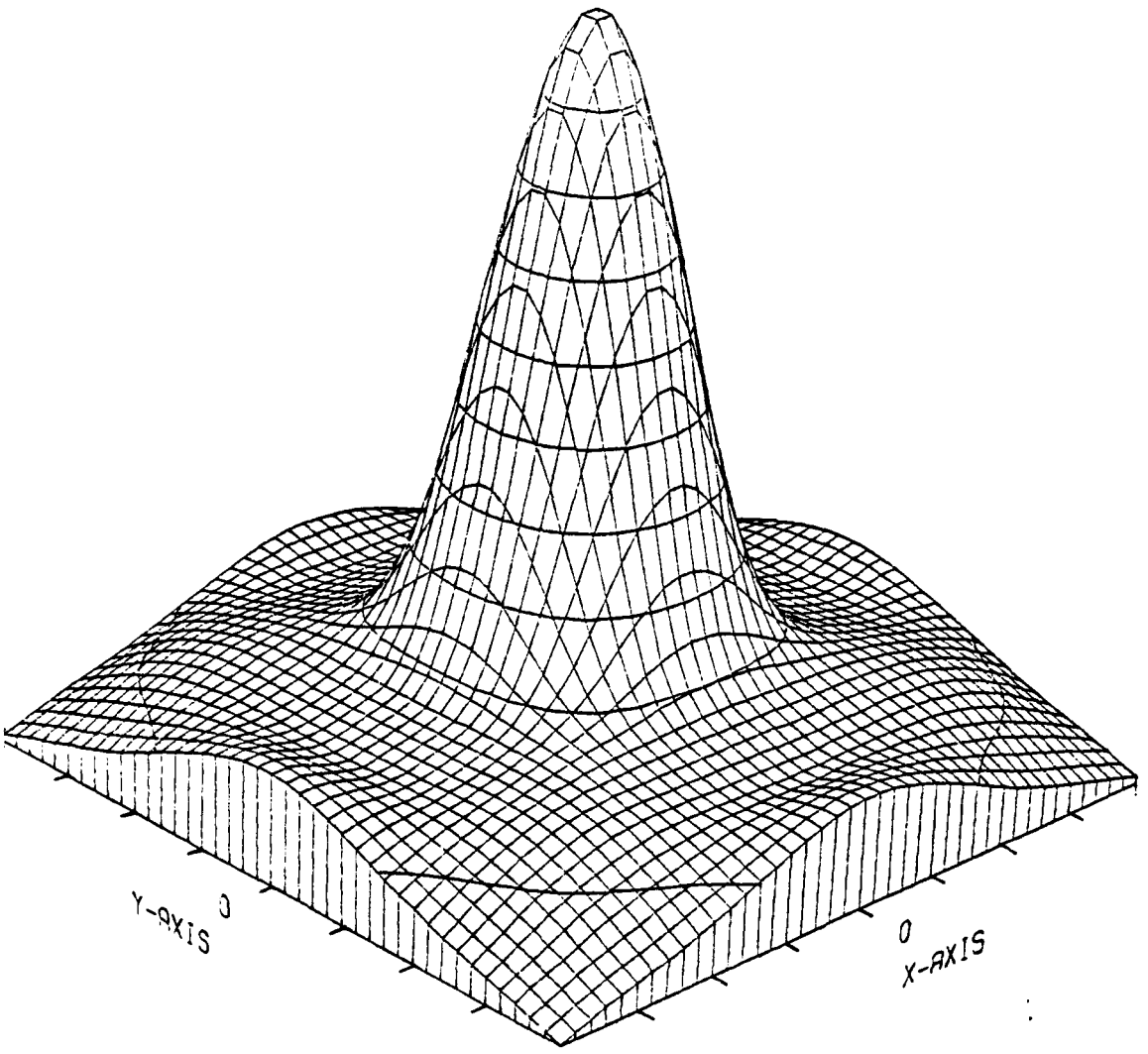

(e)

Fig. 2 (Cont'd) — Plots of the amplitude of the radiation field in the x and y plane at (a) z = 0, (b) z = 150 cm, (c) z = 300 cm, (d) z = 450 cm and (e) z = 600 cm. The tick marks are separated by a distance w_o.

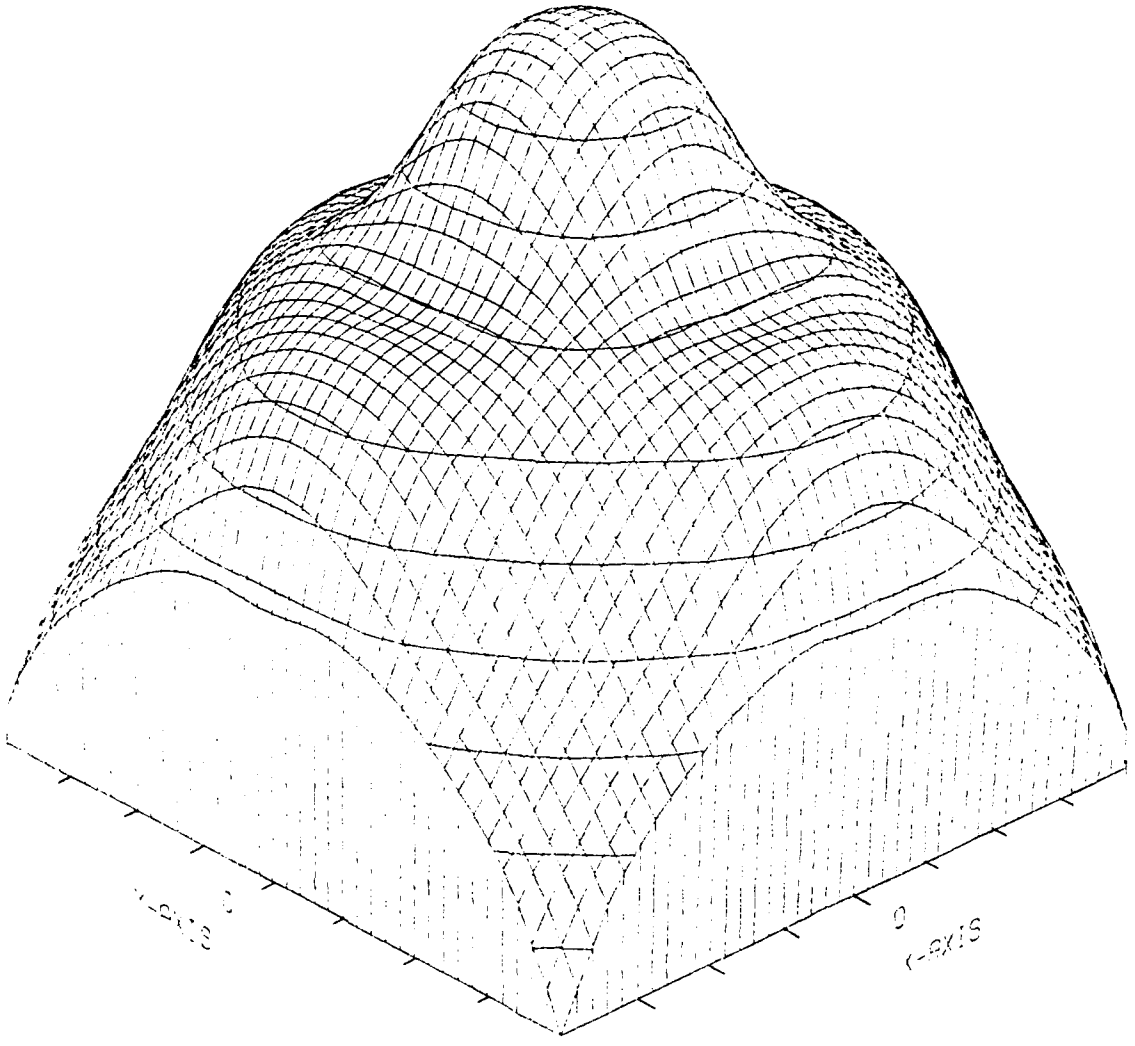

(a)

Fig. 3 — Plots of the phase of the radiation field in the x and y plane (a) z = 150 cm and (b) z = 600 cm. The tick marks are separated by a distance w_0. The discontinuity is an artifact.

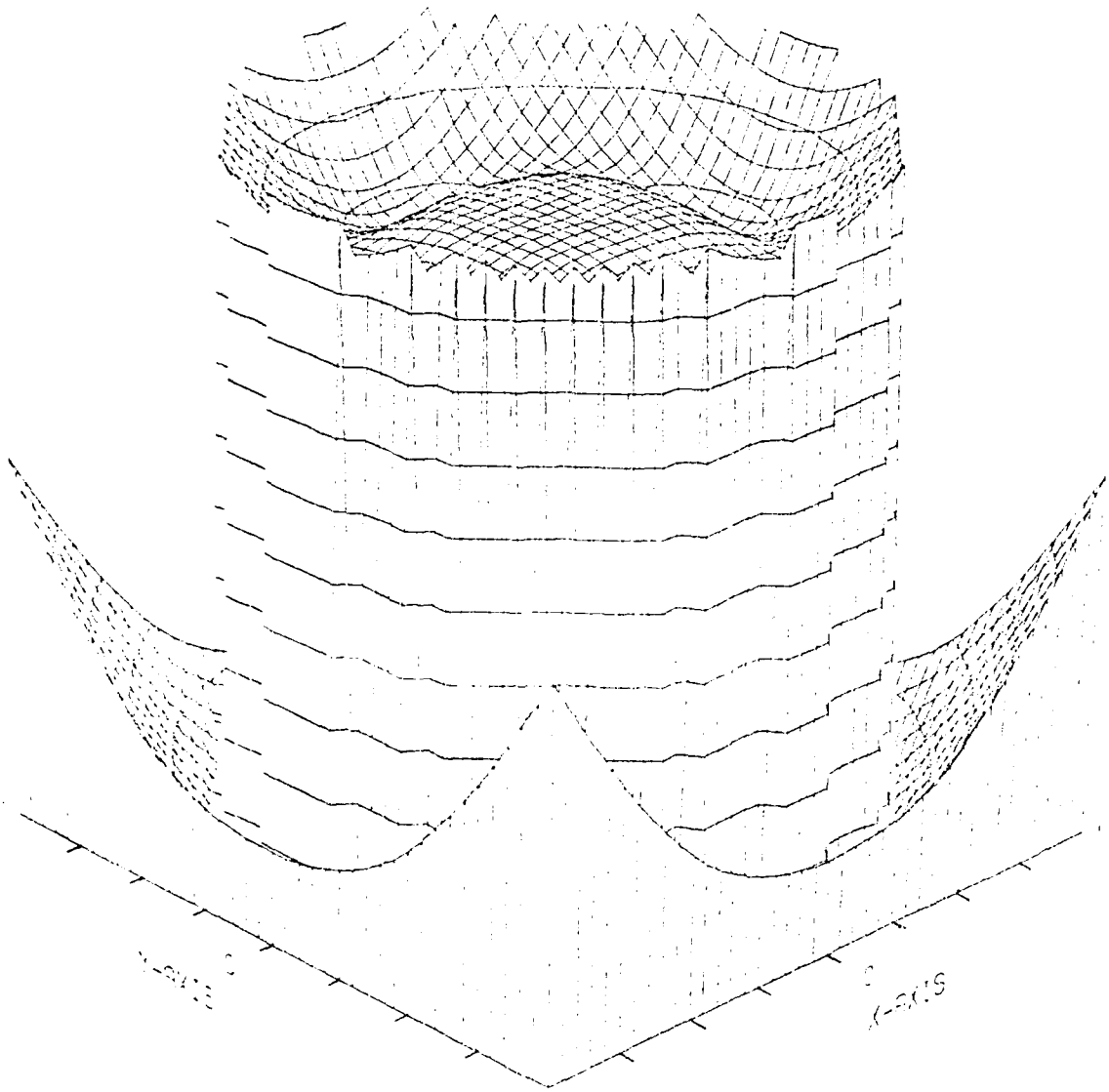

(b)

Fig. 3 (Cont'd) — Plots of the phase of the radiation field in the x and y plane at (a) z = 150 cm and (b) z = 660 cm. The tick marks are separated by a distance w_y. The discontinuity is an artifact.

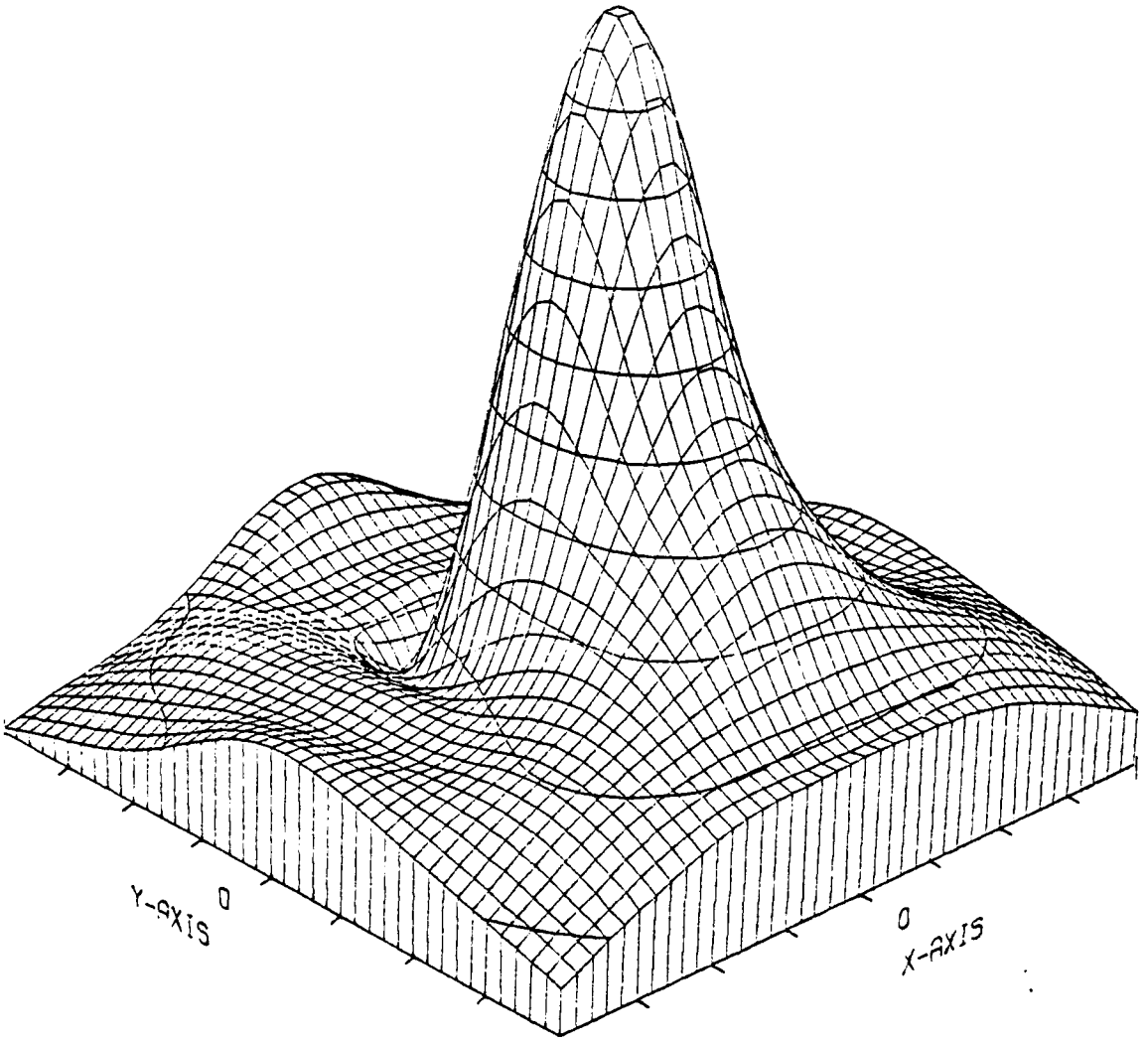

Fig. 4 — Plot of the amplitude of the radiation field in the x and y plane for the electron beam that deviated from the axis. The tick marks are separated by a distance w_o.

References

[1] C.-M. Tang and P. Sprangle, "Two-Dimensional, Semi-Analytical Formulation of the Free Electron Laser Oscillator". Proc. of the Intl. Conf. on Lasers '82. STS Press, McLean. VA. 177-186 (1982).

[2] C.-M. Tang and P. Sprangle. "Semi-Analytical Formulation of the Two-Dimensional Pulse Propagation in the Free-Electron Laser Oscillator", Free-Electron Generators of Coherent Radiation, C. A. Brau, S. F. Jacobs, M. O. Scully, Editors, Proc. SPIE 453, 11-24 (1984).

[3] P. Elleaume and D. A. G. Deacon, "Transverse Mode Dynamics in a Free-Electron Laser", Appl. Phys. B33, 9-16 (1984).

[4] L. R. Elias and J. C. Gallardo, "Cylindrical Gaussian-Hermite Modes in Rectangular Waveguide Resonators", Appl. Phys. B31, 229-233 (1983).

[5] H. P. Freund and A. K. Ganguly, "Nonlinear Theory of Ubitron/FEL Amplifier in Compton Regime", submitted to the Proceedings of Lasers 84.

[6] W. B. Colson and J. L. Richardson, "Multimode Theory of Free Electron Laser Oscillators". Phys. Rev. Lett. 50, 1050-1053 (1983).

[7] B. J. Coffey, M. Lax and C. J. Elliott, "Three-Dimensional Propagation in Free-Electron Laser Amplifiers", IEEE J. of Quantum Electronics, QE-19, 297-305 (1983).

[8] D. Quimby and J. Slater, IEEE J. of Quantum Electronics QE-19, 800 (1983).

[9] W. M. Fawley, D. Prosnitz, S. Doss and R. Gelinas, "Radially Resolved Simulation of a High-Gain Free Electron Laser Amplifier", Free-Electron Generators of Coherent Radiation, C. A. Brau, S. F. Jacobs, M. O. Scully, Editors, Proc. SPIE 453, 212-217 (1984).

[10] L. R. Elias and J. C. Gallardo, "Coherent Lienard-Wiechert Fields Produced by Free-Electron Lasers", Phys. Rev., A24, 3276-3279 (1981).

[11] N. M. Kroll and M. N. Rosenbluth, "Sideband Instabilities in Trapped Particle Free-Electron Lasers", Free Electron Generator of Coherent Radiation, Physics of Quantum Electronics, Vol. 7, Addison-Wesley, Reading, MA. 147-174 (1980).

[12] J. C. Goldstein and W. B. Colson, "Control of Optical Pulse Modulation due to the Sideband Instability in Free Electron Lasers", Proc. of the Intl. Conf. on Lasers '82.

R. C. Powell, Editor, STS Press, McLean, VA, 218-225 (1982).

[13] P. Sprangle and C.-M. Tang, "Three-Dimensional Nonlinear Theory of the Free-Electron Laser," Appl. Phys. Lett. 39, 677-679 (1981).

[14] C.-M. Tang and P. Sprangle, "The Three-Dimensional Non-Linear Theory of the Free-Electron Laser Amplifier", Free-Electron Generators of Coherent Radiation, Physics of Quantum Electronics. Vol. 9, S. F. Jacobs, G. T. Moore, H. S. Pilloff, M. Sargent III, M. O. Scully and R. Spitzer, Editors, Eddison-Wesley Publ. Co., Reading, MA, 627-650 (1982).

[15] N. S. Ginzburg, "Self-Focusing Effects in Free Electron Lasers", Optical Communications, 43, 203-206 (1982).

[16] N. S. Ginzburg, N. F. Kovalev and N. Yu. Rusov, "Electron-Diffractional Mode Selection in Free Electron Lasers", Optical Communications, 46, 300-304 (1983).

[17] E. T. Scharlemann, A. M. Sessler, and J. S. Wurtele, "Optical Guiding in a Free Electron Laser", Submitted to the Workshop on Coherent/Collective Propagation of Relativistic Electron-Beams/Electromagnetic Radiation Villa Olmo, Como, Italy, Sept. 13-16, 1984.

[18] S. Benson, private communications.

END

FILMED

2-86

DTIC